Vibrational Spectra and Molecular Orientation with Experimental Configuration Analysis in Surface Sum Frequency Generation (SFG)†

ARTICLE *in* THE JOURNAL OF PHYSICAL CHEMISTRY C · MARCH 2007

Impact Factor: 4.77 · DOI: 10.1021/jp067062h

5 AUTHORS, INCLUDING:

Wei Gan
Chinese Academy of Sciences
31 PUBLICATIONS **1,220** CITATIONS
SEE PROFILE

Zhen Zhang
Max Planck Institute for Polymer Research
20 PUBLICATIONS **626** CITATIONS
SEE PROFILE

Yuan Guo
Chinese Academy of Sciences
37 PUBLICATIONS **590** CITATIONS
SEE PROFILE

Hong-fei Wang
Pacific Northwest National Laboratory
56 PUBLICATIONS **1,708** CITATIONS
SEE PROFILE

Vibrational Spectra and Molecular Orientation with Experimental Configuration Analysis in Surface Sum Frequency Generation (SFG)†

Wei Gan,‡,§ Bao-hua Wu,‡,|| Zhen Zhang,‡ Yuan Guo, and Hong-fei Wang*

State Key Laboratory of Molecular Reaction Dynamics, Institute of Chemistry, the Chinese Academy of Sciences, Beijing, China, 100080

Received: October 27, 2006; In Final Form: January 27, 2007

Recent developments in sum frequency generation-vibrational spectroscopy (SFG-VS) have shown that SFG-VS is not only a spectroscopic probe of the molecular interfaces but also an important tool for studying molecular spectroscopy in general. It has been demonstrated that through polarization and symmetry analysis a few sets of polarization selection rules can explicitly help the vibrational spectral assignment. This worked because of the coherent nature and the strong orientational dependence of the SFG process from the molecular interfaces or films. In this work, we further discuss the dependence on the experimental configurations in the SFG-VS polarization analysis. Such experiment and analysis can further increase the ability of the SFG-VS as the tool for discerning spectral details and overlapping spectral features, as well as the ability to obtain detailed molecular orientational information. The experimental configuration dependence of the SFG spectra is most significant in the ppp polarization combination, less significant in the sps and ssp polarization combinations, due to the fact that ppp is the result of the combination of four different susceptibility tensor elements, while both ssp and sps are of a single tensor element. Such complexity of the ppp spectrum, which is very useful as demonstrated in this work, used to be avoided in the SFG-VS studies. The spectral details of the SFG-VS from the vapor/methanol, vapor/ethanol, and vapor/ethylene glycol interfaces are studied in different experimental configurations. The strong experimental configuration dependence observed for these liquid interfaces also indicated that they possess well-ordered interfacial structures. The concepts and conclusions in this report may find future applications in studying more complex molecular interfaces and films.

1. Introduction

In the past two decades, second harmonic generation (SHG) and sum frequency generation-vibrational spectroscopy (SFG-VS) have been employed as effective surface probes for their unique surface sensitivity and surface selectivity, especially for the investigation of liquid interfaces.[1−6] Recent developments in SFG-VS have increasingly shown that SFG-VS is also an important tool for understanding molecular vibrational spectroscopy, which employs the interface as the ideal sample of the molecularly thin and oriented layer of molecules for polarization measurement.[7−10] Quantitative measurement and interpretation of the molecular orientation and vibrational spectra at the molecular interfaces can be achieved through systematic polarization and molecular symmetry analysis in SHG and SFG.[10−12] Thus, a few sets of polarization selection rules were derived for the methyl, the methylene and methine groups at liquid and material interfaces, and their SFG spectra, congested with the overlapping symmetric stretching modes, asymmetric stretching modes, Fermi resonance as well as other combinational modes were also explicitly assigned.[7−10] One clear advantage of the polarization selection rules in SFG-VS is that some ambiguous or incorrect assignments can be directly clarified.[7−10] These developments have led us to the novel perspective that the SFG-VS technique can be employed as a powerful tool to study molecular vibrational spectroscopy by employing its intrinsically coherent nature and strong polarization dependence.[9,10] Through systematic polarization and symmetry analysis, more accurate information on molecular orientation, structure, and dynamics can also be obtained,[13−17] especially with the knowledge on the correctly assigned SFG-VS spectra.[7−10,13]

The successful development in the polarization analysis also provides tools for the analysis of the neglected dimension in the SFG-VS studies[10] through the strong experimental configuration dependence of the SFG-VS spectra. As pointed out in previous studies,[7,8,10] because of such experimental configuration dependence, the polarization selection rules developed from the liquid interfaces and molecular films in the copropagating geometry need further examination when the experimental configuration is varied significantly. For example, polarization selection rules may change for the metal or semiconductor interfaces or may change under the total internal reflection (TIR) experimental configuration or counter-propagating experimental configuration.[7,10] Besides, it has long been noticed that in the literature the SFG-VS spectra in the same polarization combination differed significantly for the same molecular interface when

† Part of the special issue "Kenneth B. Eisenthal Festschrift".

* Author to whom correspondence should be addressed. E-mail: hongfei@iccas.ac.cn. Tel: 86-10-62555347. Fax: 86-10-62563167.

‡ Also graduate students of the Graduate School of the Chinese Academy of Sciences.

§ Current address: Department of Biological Sciences and Department of Chemistry, Columbia University, 2960 Broadway, New York, NY, 10027.

|| Current address: Department of Chemistry, Emory University, 1515 Dickey Drive Atlanta, GA.

10.1021/jp067062h CCC: $37.00
Published on Web 03/23/2007

being measured by different research laboratories. Because we have examined these data case by case, we have realized that many of the differences can be attributed to the differences in the experimental configurations used, as long as the data are reproducible.[10,13,14,18] These included SFG-VS spectra of some very extensively investigated interfaces, such as the vapor/water interface,[4,5,13,14,18−20] the vapor/poly(methyl methacrylate)-(PMMA) interface,[21,22] the vapor/ethanol interface,[8−10,23,31] the vapor/methanol interface,[10,24−31] and the vapor/ethylene glycol interface.[7,10,32] All such "inconsistencies" due to the differences of experimental configuration in the SFG-VS studies certainly require further studies.

The influence of the experimental configuration in the SHG has been studied as early as 1985 by Dick et al.[33] However, experimental configuration analysis has seldom been employed except for a few cases in SHG and SFG-VS studies.[33−35] Recently, there was a report on the determination of the surface refractive index with two experimental configurations in SFG-VS.[22] Our research group recently discussed the dependence of the accuracy of the polarization null angle (PNA) method, as well as polarization spectra of the vapor/water interface in different experimental configurations.[13,14,36]

In the latter study, we found that by carefully varying the incident angle of the visible laser beam in the SFG experiment by less than 20°, the ppp spectral intensity of the 3700 cm^{-1} peak of the neat vapor/water interface can be varied by more than 2 orders of magnitude.[13,14] With these experimental data, unique orientational structure and dynamics information of the free O−H group at the air/water interface were determined. Here, as usually used in the SFG-VS studies, the three letter indexes, such as ssp, ppp, and sps, denote the experimental polarization combinations of the SFG signal, visible (vis) and infrared (IR) light, respectively, with *p* as the polarization direction within the incident plane and *s* as the polarization perpendicular to it. This detailed study convinced us that systematic studies on the dependence of the ppp, as well as ssp and sps SFG-VS spectrum on experimental configuration, can provide novel information on the details of molecular vibrational spectra and on the determination of molecular orientational structure and dynamics at the interface. However, in SFG-VS studies, the relationship between the experimental configuration and polarization analysis has not been fully explored, and the applications of such analysis are yet to be systematically pursued.

Besides the most popularly used SFG experimental configuration where the visible and infrared laser beams are from the rare phase (generally the air phase) and the SHG/SFG signal is detected in the reflection direction or transmission direction,[37,38] total internal reflection (TIR) configuration was also used to detect the SFG signal.[39−43] In the TIR case, the SFG signal can be enhanced by as much as 2 or 3 orders of magnitude because of the favorable Fresnel factors from total internal reflection.[33,39,44] Proposal of an internal−external reflection configuration in SFG-VS was also reported recently.[45] However, in these studies, the main concern was to improve signal intensity other than performing polarization analysis of the vibrational spectra. As one can expect, in measurement with TIR geometry, the ppp SFG-VS intensity is usually much stronger than that in all other polarization combinations including the ssp; one may surmise that configuration analysis should be even more crucial than non-TIR geometry.

In this work, we intend to study the experimental configuration dependence of the SFG-VS spectral intensities at different incident angles of the fundamental laser beams. With experimental configuration analysis together with polarization analysis, we studied the SFG-VS spectral details, as well as molecular orientation, of the vapor/methanol (CH_3OH), vapor/ethanol(CH_3CH_2OH), and vapor/ethylene glycol ($HOCH_2CH_2OH$) interfaces.

Simulation of the SFG-VS intensity dependence of the CH_3-symmetric stretching mode (CH_3-SS) of the methanol molecule at the vapor/methanol interface in the ssp, ppp, and sps polarization combinations on the visible and IR incident angles provided us a way to map out the missing spectral peaks in the ppp polarization combination. The prediction was confirmed with the expected experimental configuration. This clearly indicates the effectiveness of the model for quantitative simulation and calculation of the SFG-VS spectra from the empirical parameters for the vapor/methanol interface, including the hyperpolarizability tensor ratios, the interfacial local field factors, and so forth.[10,36,46,47] Simulation predictions of the SFG-VS intensity dependence of the CH_3-SS, CH_3-SS-Fermi, and CH_3-AS modes of the ethanol molecule at the vapor/ethanol interface, and the CH_2-SS, CH_2-SS-Fermi, and CH_2-AS modes of the ethylene glycol (EG) molecule at the vapor/EG interface in the ssp, ppp, and sps polarization combinations on the visible and the IR incident angles were also confirmed by the experimental observation. Because not only the polarization dependence but also the experimental configuration dependence of the SS and AS modes is significantly different, these observations provided further evidence to make unambiguous assignments of the SFG-VS vibrational spectra. As we have demonstrated, the previous assignments of ethanol and EG C−H stretching vibrational modes were with significant mistakes.[7−9]

There are remarkable differences between the SFG-VS and the normal infrared and Raman spectroscopy. Unlike the normal IR and Raman techniques, the SFG-VS signal originates from a coherent process in which coherent interference effects between the contributions from different molecular groups as well as from the different vibrational modes of the same molecular group are ubiquitous. With the control of the experimental configuration, the intensity as well as the phase relationship between the different SFG-VS spectral features in the same polarization varies in certain ways and they can be calculated and simulated from the known hyperpolarizability tensors and the molecular symmetry information.[10] In contrast, normal Raman and IR spectroscopy are incoherent processes, and no spectral interference effect can be observed. Even though there can be some polarization dependence in the Raman spectroscopy for both isotropic and ordered molecular systems and in the infrared spectroscopy for the ordered molecular systems, and such dependence has been used to deduce molecular orientation information in molecular films, normal Raman and IR spectroscopy are not able to provide spectral details as the SFG-VS, or other coherent spectroscopic techniques.[48,49] This is why we intend to demonstrate that active control and analysis of the experimental configuration dependence in the SFG-VS studies can make SFG-VS an even more effective spectroscopic tool for complex molecular spectroscopy and interface studies.

Using the SFG-VS, the strong experimental configuration dependence observed for the liquid interfaces studied also indicates that these interfaces possess well-ordered interfacial orientational structures. The concepts and conclusions on combining experimental configuration analysis with the polarization analysis in the SFG-VS, as well as other coherent nonlinear spectroscopic techniques, may find further applications for the investigation of the ordered molecular systems.

2. Polarization and Experimental Configuration Analysis

2.1. Basic SFG-VS Theory. The SFG intensity reflected from an interface can be expressed as a square function of the effective sum frequency susceptibility $\chi^{(2)}_{\text{eff}}$.[7,37]

$$I(\omega) = \frac{8\pi^3\omega^2 \sec^2\beta}{c^3 n_1(\omega)\, n_1(\omega_1)\, n_1(\omega_2)} |\chi^{(2)}_{\text{eff}}|^2 I(\omega_1)\, I(\omega_2) \qquad (1)$$

As defined previously,[10] c is the speed of the light in the vacuum; ω, ω_1, and ω_2 are the frequencies of the SFG signal, visible, and IR laser beams, respectively; $n_j(\omega_i)$ is the refractive index of the bulk medium j at the frequency ω_i, and $n'(\omega_i)$ is the effective refractive index of the interface layer at ω_i; β_i is the incident or reflect angle from the interface normal of the ith light beam (normally β_1 for the visible laser and β_2 for the infrared laser); and $I(\omega_i)$ is the intensity of the SFG signal or the input laser beams, respectively.

For a rotationally isotropic liquid interface ($C_{\infty v}$), $\chi^{(2)}_{\text{eff}}$ are related to the seven nonzero macroscopic susceptibility tensors and can be expressed into the linear combination of the following four independent experimentally measurable terms.[10]

$$\chi^{(2),\text{ssp}}_{\text{eff}} = L_{yy}(\omega)\, L_{yy}(\omega_1)\, L_{zz}(\omega_2) \sin\beta_2 \chi_{yyz}$$

$$\chi^{(2),\text{sps}}_{\text{eff}} = L_{yy}(\omega)\, L_{zz}(\omega_1)\, L_{yy}(\omega_2) \sin\beta_1 \chi_{yzy}$$

$$\chi^{(2),\text{pss}}_{\text{eff}} = L_{zz}(\omega)\, L_{yy}(\omega_1)\, L_{yy}(\omega_2) \sin\beta \chi_{zyy}$$

$$\begin{aligned}\chi^{(2),\text{ppp}}_{\text{eff}} = & -L_{xx}(\omega)\, L_{xx}(\omega_1)\, L_{zz}(\omega_2) \cos\beta \cos\beta_1 \sin\beta_2 \chi_{xxz} \\ & - L_{xx}(\omega)\, L_{zz}(\omega_1)\, L_{xx}(\omega_2) \cos\beta \sin\beta_1 \cos\beta_2 \chi_{xzx} \\ & + L_{zz}(\omega)\, L_{xx}(\omega_1)\, L_{xx}(\omega_2) \sin\beta \cos\beta_1 \cos\beta_2 \chi_{zxx} \\ & + L_{zz}(\omega)\, L_{zz}(\omega_1)\, L_{zz}(\omega_2) \sin\beta \sin\beta_1 \sin\beta_2 \chi_{zzz}\end{aligned} \qquad (2)$$

It is so defined that the xy plane in the laboratory coordinates system $\lambda(x,y,z)$ is the plane of the interface, with z is the interface normal; L_{ii} ($i = x,y,z$) is the Fresnel coefficient determined by the refractive indexes of the two bulk phase, the effective refractive index of the interface layer, and the incident and the reflected angles.[10,37,50] $\chi^{(2)}_{ijk}$ tensors are related to the molecular hyperpolarizability tensor $\beta^{(2)}_{i'j'k'}$ in the molecular coordinates system $\lambda'(a,b,c)$ through the ensemble average over all of the possible molecular orientations, and this can be described as[10,37,50]

$$\chi^{(2)}_{ijk} = N_s \sum_{i'j'k'} \langle R_{ii'} R_{jj'} R_{kk'} \rangle \beta^{(2)}_{i'j'k'} \qquad (3)$$

where N_s is the number density of the interface moiety under investigation and $R_{\lambda\lambda'}$ is the element of the Euler rotational transformation matrix from the molecular coordinates $\lambda'(a,b,c)$ to the laboratory coordinates λ (x,y,z).[51,52] The expressions of the relationship between the $\chi^{(2)}_{ijk}$ tensor and the microscopic (molecular) hyperpolarizability tensor $\beta^{(2)}_{i'j'k'}$ for the molecular groups with C_{2v}, C_{3v}, and $C_{\infty v}$ symmetry have been described in literature.[7,8,10,27,53−55] Thus, molecular groups investigated in SFG-VS, such as CH_3-, -CH_2-, CH, -CO, -CN, -OH groups, and so forth, can be treated easily.

The polarization dependence analysis in SFG-VS was based on eq 2, and the symmetry analysis was based on eq 3.[10] In eq 2, the $\chi^{(2),\text{ppp}}_{\text{eff}}$ term has a complex relationship with the Fresnel factors. The above brief discussion forms the basis of the experimental configuration analysis in this paper.

2.2. Idea of Experimental Configuration Analysis. As shown in eq 2, the analysis of the experimental configuration dependence of the SFG-VS spectra is theoretically trivial.[10,37] However, the idea to employ it systematically in SFG-VS studies as a spectroscopic tool is novel and ought not to be slighted.

The experimental configuration dependence comes in through the change of the Fresnel factors associated with each second-order susceptibility tensor element. Therefore, as described below, for ssp, sps, and pss polarization combination measurements, even though the total intensity may vary in different experimental configurations according to the corresponding Fresnel factors, the relative intensity between different spectral features in the same spectra remains essentially the same (because in these polarization combinations, only one macroscopic susceptibility tensor element is responsible for each, that is, χ_{yyz} for ssp, χ_{yzy} for sps, and χ_{zyy} for pss). However, in the ppp polarization combination, because it is the sum of four different macroscopic susceptibility tensor elements, namely, χ_{xxz}, χ_{xzx}, χ_{zxx}, and χ_{zzz}, the change of the experimental configuration can significantly change the relative values of the Fresnel factors associated with each of the four susceptibility tensor elements. Therefore, not only the intensity but also the relative phase (sign) of the contributions from these four elements can be significantly changed. Besides, because different molecule groups and different vibrational modes of the same molecular group can all contribute to the macroscopic susceptibility tensor element, varying the experimental configuration can result in very complex behaviors in the ppp SFG-VS spectra. This was partly the reason that in the SFG-VS literature people generally concentrated on analyzing the ssp and sps spectra and avoided analyzing the more complex ppp spectra.

Theoretically, the key to understanding the experimental configuration dependence of the complex behaviors in the ppp SFG-VS spectra lies in the analysis of the relative contributions from the different groups and different vibrational modes. In the SFG-VS polarization analysis, a few sets of polarization selection rules were concluded because the polarization dependence is rooted in the intrinsic symmetry of different groups and different vibrational modes.[7,8,10] The experimental configuration dependence is rooted similarly. Changing the experimental configuration can tune the relative contributions to the total SFG-VS field from the different molecular groups and different vibrational modes. Thus, this is a way of distinguishing and identifying the symmetry properties of each of the overlapping spectral features and to quantitatively evaluate their relative contributions in the SFG-VS spectra. In practice, this can become very useful for the SFG-VS spectral analysis, in addition to the recently developed polarization analysis methodologies.[7−10,56]

Experimentally, the interference effects and phase changes in the ppp polarization combination under different experimental configurations can be observed and evaluated easily. Generally, spectral fitting in SFG-VS can give good agreement on the relative phases (signs) for different spectral features, unless the spectral quality is generally poor and no spectral detail can be discerned.[57,58] The absolute phases (signs) for different spectral features can also be measured.[59] Therefore, controlling the relative phase of the different spectral features in the ppp polarization combination in SFG-VS can be a very useful way of discerning different spectral features, and such an approach can be achieved by systematically varying the experimental configuration. More quantitative applications can be achieved

by applying mathematical analysis to such data using either the mapping approach or the singular-value decomposition (SVD) method and so forth.[56,60,61]

2.3. Simulation of CH_3-SS Vibration Mode at Vapor/Methanol Interface. Through theoretical simulation, experimental configuration can be optimized to help design the SFG-VS experimental conditions for the observation of a specific spectral feature in the ppp polarization combination. Here we choose the CH_3-SS vibrational mode at the vapor/methanol interface to illustrate this point. Recently, we studied the sensitivity of the polarization null angle (PNA) method and compared the accuracy of the PNA method with the traditionally used intensity ratio method for the determination of the orientational parameter in different experimental configurations.[36,55]

In order to choose a proper experimental configuration for polarization analysis, it is necessary to know the change of the SFG intensity with the change of the experimental configuration. All of the formulas used in this simulation were standard in the recent literature.[10] The issues concerning the accuracy and reliability of these parameters were discussed thoroughly in the recent literature,[10] and the quantitative and empirical corrections of these parameters were also discussed and tested in detail recently.[46] Our simulation showed that besides the experimentally determined parameters the uncertainty of all of the uncertain parameters were usually very limited in order to be consistent with the apparent trends in the experimental data in different polarization combinations and experimental configurations. This certainly assured the robustness of the simulation and the conclusions that followed.

The parameters used in the simulation are as follows. The hyperpolarizability ratios are $R = \beta^{(2)}_{aac}/\beta^{(2)}_{ccc} = \beta^{(2)}_{bbc}/\beta^{(2)}_{ccc} = 1.7$.[10] The refractive index is set as 1.0 in the air and 1.33 in the bulk methanol for all of the fundamental laser beams and SFG signal. The refractive index at the interface is 1.15, calculated with the equation presented by Shen et al.[10,37] Assuming that the tilt angle of the methyl group is close to the surface normal, the results of the simulation on experimental configuration are plotted in Figure 1. Here we use $\theta = 10°$ instead of $\theta = 0°$. The latter value is the measured methyl tilt angle.[55,36] When $\theta = 0°$, the sps intensity is a constant zero in all different experimental configurations. So we use the $\theta = 10°$ data to show the experimental configuration dependence of the sps intensity when θ is close to 0°. In doing so, the ssp and ppp curves are only slightly different from the case for $\theta = 0°$ because both ssp and ppp SFG-VS intensity here are almost insensitive to the θ within the 0° −10° range, which is within the orientationally insensitive region for the ssp and ppp intensities.[10,11]

Several conclusions can be readily deduced from the simulation in Figure 1:

(*a*) *sps(pss) intensity is always very small in comparison with that of ssp or ppp.*

(*b*) *ssp and ppp intensities are both small with large* β_2 (*near glazing incidence) or small* β_2 (*near perpendicular incidence).*

(*c*) *ssp intensity is always small with large* β_1.

(*d*) *ppp intensity generally has a zero (null) value at certain* β_1, *and becomes larger and larger when* β_1 *becomes smaller.*

(*e*) *sps(pss) intensity is always small with large* β_2, *and small with large or small* β_1.

(*f*) *ssp and ppp intensities are the largest around* $\beta_2 = 50°$ *at a given* β_1; *while the sps(pss) intensity is the largest around* $\beta_1 = 50°$ *at a given* β_2.

Here each pair of the β_1 and β_2 values specifies a unique experimental configuration. These conclusions may vary from

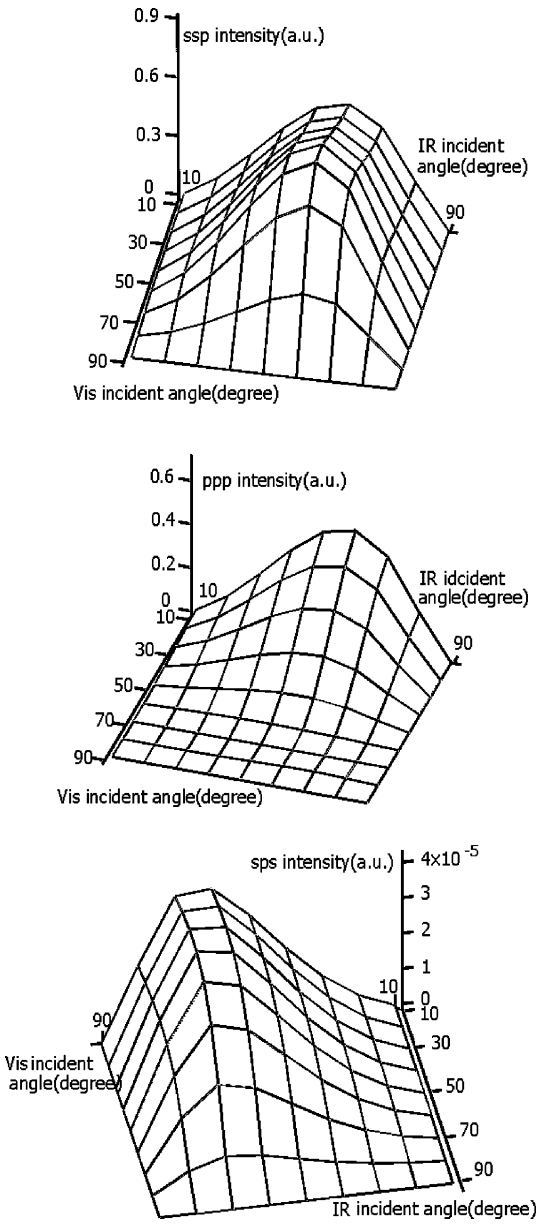

Figure 1. Simulation of the *ssp* (top), *ppp* (middle), and *sps* (bottom) intensities for the CH_3-SS mode of the vapor/methanol interface with different visible and IR incident angles. The orientational angle of the methyl groups are set as 10°. Using this angle makes the sps intensities nonzero, but still very small.

those for the interfacial molecules with significantly different orientation angles, the other symmetry category such as C_{2v} symmetry, the AS modes of these molecular groups, and the $C_{\infty v}$ symmetry with a hyperpolarizability ratio R less than 1. Nevertheless, from our simulation, features in *c*, *e*, and *f* kept true in many cases. Such simulation is straightforward once the range of the key parameters is determined. Therefore, simulation on other cases is not presented here.

The conclusion in *f* provides the rationale for why most of the SFG-VS experiment was performed around $\beta_2 = 50°$. With a fixed β_2, the value of β_1 can make a significant difference. As shown in Figure 2 (top), when $\beta_2 = 52°$, the intensity ratio between ssp and ppp polarization combination changes dramatically with β_1. Simulation showed that this ssp/ppp ratio is not very sensitive to the change of β_2. According to the simulation in Figure 2 (top), if β_1 is smaller than 40° then the ppp intensity gradually becomes comparable to that of the ssp intensity. Two small peaks in the ppp polarization were indeed observed

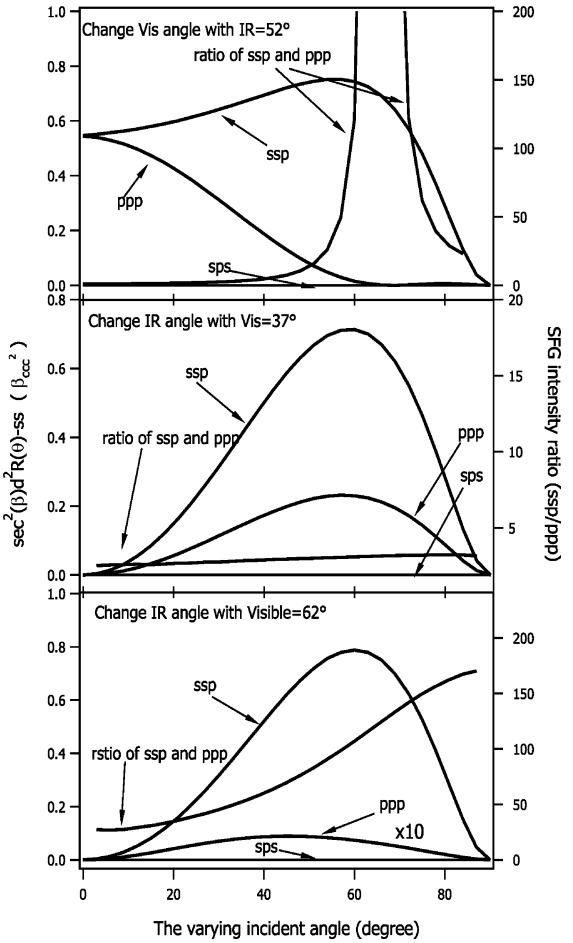

Figure 2. Simulation of the SFG intensity dependence of the CH_3-SS mode at the vapor/methanol interface with the change of the incident angle for the visible laser beam (top) or the IR laser beam (middle and bottom). The factor $1/\cos^2 \beta$ in eq 1 was also included for comparison of the SFG intensity between experimental configurations.

experimentally as shown in Figure 3 when $\beta_1 = 37°$. In comparison, when $\beta_1 = 62°$, these ppp peaks disappeared into the noise level. It is very important that the experimental results followed the simulation quite accurately. This indicated that not only the formulation used for the simulation is sound but the parameters used in the simulation are also accurate. In comparison, the less-sensitive intensity dependence of the ssp versus ppp ratio on β_2 is best illustrated in Figure 2 (middle, bottom). Using such simulations, optimal experimental configurations for observing specific spectral features can be predicted.

The simulations in this work are carried out in the copropagation experiment geometry. Some aspects on the differences between this experimental geometry and counterpropagation geometry were discussed previously.[7,8,10] The procedures in this work are applicable to the experimental configuration of other categories, such as counterpropagation geometry or TIR geometry.

In a given experimental configuration, the formulation with the *general orientational parameter c* and the *susceptibility strength factor d* in different polarization combinations is very useful for understanding the polarization and orientational dependence of the SFG-VS field strength or intensity.[7,8,10,11] As shown previously, any $\chi^{(2)}_{\text{eff}}$ in eq 1 can be simplified into the following form[11]

$$\chi^{(2)}_{\text{eff}} = N_s\, d(\langle\cos\theta\rangle - c\langle\cos^3\theta\rangle) = N_s\, dr(\theta) \qquad (4)$$

Then eq 1 is factorized into

$$I(\omega) = Ad^2\, R(\theta) N_s^2\, I(\omega_1)\, I(\omega_2) \qquad (5)$$

$$R(\theta) = |r(\theta)|^2 = |\langle\cos\theta\rangle - c\langle\cos^3\theta\rangle|^2 \qquad (6)$$

Here $r(\theta)$ is called the *orientational field functional*, which contains all molecular orientational information at a given SFG experimental configuration. As shown below, we shall use the calculated c and d values to evaluate the relative SFG field strength and the phase of the SFG-VS intensity in different polarization combinations, and their dependence on the orientation of a particular molecule group.[7,8,10,11]

3. Experimental Section

The experiment setup has been described elsewhere.[7,8] Briefly, the 10 Hz and ~23 ps SFG spectrometer laser system from EKSPLA was set in a copropagating configuration. Some SFG polarization optics were rearranged from the original design to improve the polarization control in SFG experiment.[55] The visible wavelength is fixed at 532 nm, and the full range of the IR tunability is from 1000 to 4300 cm^{-1}. The specified spectral resolution of this SFG spectrometer is <6 cm^{-1} in the whole IR range and about 2 cm^{-1} around 3000 cm^{-1}. The turning of the infrared laser was set at 5 cm^{-1} increments for the vapor/methanol case and 2 cm^{-1} increments for the vapor/ethanol and vapor/EG cases. Each scan was averaged over 100 laser pulses per point. The energy of the visible beam is typically less than 300 microjoules, and that of the IR beam is less than 200 microjoules.

In this work, the incident angles of the visible and IR laser beams were changed to get different experimental configurations. All measurements were carried out at controlled room temperature (22.0 ± 0.5 °C). The liquid samples were obtained from Fluka: methanol (> 99.8%), ethanol (> 99.8%), ethylene glycol (99%). All liquid samples were housed in a round Teflon beaker (diameter ~5 cm) for SFG measurement. The complete experimental setup on the optical table was covered in a plastic housing to reduce the air flow.

4. Results and Discussions

4.1. Seeing Unseen Spectral Features at Vapor/Methanol Interface. The SFG spectra of the vapor/methanol interface were measured in two experimental configurations, that is, configuration I, $\beta_1 = 62°$ and $\beta_2 = 53°$; configuration II, $\beta_1 = 37°$ and $\beta_2 = 51°$.[10,36] The SFG spectra in *ssp*, *sps*, and *ppp* polarization combination are shown in Figure 3.

The observed spectra in Figure 3 agree well with the simulation in section 2.3. The almost zero peak intensities with configuration I at the 2928 and 2940 cm^{-1} peak positions in the ppp polarization combination become apparent, and their relative intensity is in proportion in the ppp polarization combination with configuration II. The concurrence of these two peaks also confirms the fact that they belong to the same molecular symmetry.[8,10]

Using the *general orientational parameter c* and the *susceptibility strength factor d* formulation, the SFG-VS field strength that is proportional to $\sec(\beta)\ dr(\theta)$ is plotted against the orientational angle for the CH_3-SS and CH_3-AS modes of the vapor/methanol interface, shown in Figure 3. The d and c values used are calculated and listed in Table 1. (Because the CH_3AS mode is generally considered doubly degenerate as discussed previously,[8] the d values for the CH_3-AS mode listed here are twice as large as the values presented in previous reports, where

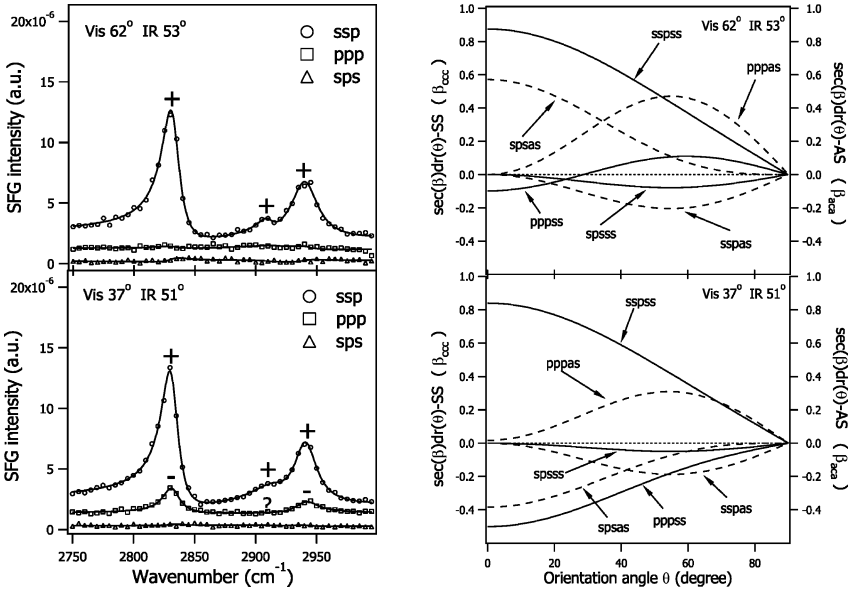

Figure 3. Left: SFG-VS spectra of the vapor/methanol interface in two experimental configurations. The solid lines are fittings with the Lorentzian line shapes. The phase of each fitted peak is marked near the spectral peak position. The ? sign indicates that the peak is at the noise level, and its sign cannot be identified explicitly. Right: simulation of the SFG-VS intensity for the CH_3-SS and CH_3-AS modes from the vapor/ethanol interface in different orientational angles. The factor sec(β) in eq 1 was included for comparison of the SFG-VS strength and phase in different experimental configurations.

TABLE 1: *c* and *d* Values for the CH_3-SS and CH_3-AS Modes at the Vapor/Methanol Interface in Both Experimental Configuration I and Experimental Configuration II

polarization		sspss	pppss	spsss	sspas	pppas	spsas
vis 62, IR 53	*c*	−0.26	1.3	1	1	1.0	∞
	d	0.34	0.16	−0.10	−0.25	0.61	−0.28 (*d*•*c*)
vis 37, IR 51	*c*	−0.26	−1.3	1	1	0.98	∞
	d	0.52	−0.17	−0.10	−0.38	0.61	−0.29 (*d*•*c*)

[a] The notation such as sspss denotes the SS mode in ssp polarization. The *d* value bears the unit β_{ccc} for the SS mode and β_{aca} for the AS mode. The parameters without two effective figures are exact values.

the values were for only one of the degenerate modes.[8,10] In the plots in the previous reports, the degeneracy was already included.[8,10] The *d* values calculated from eq 28 in the previous report[10] already included the degeneracy of the CH_3-AS mode. Careful readers may notice this difference. In order not to cause any possible confusion, from now on, we shall list the *d* value for the CH_3-AS mode as calculated from eq 28 instead of the single-mode values.) Using the *c* and *d* formulation, the orientational contribution to the SFG-VS intensity and phase from the orientational functional $r(\theta)$ can be decoupled from other factors.

The plot readily explains the appearance of the 2928 and 2940 cm^{-1} peaks in the ppp polarization combination in configuration II. This is simply because both peaks belong to the SS mode. According to the plot in Figure 3, the intensity of these two peaks should be about 25 times stronger in configuration II than in configuration I, when the tilt angle of the methyl group is about $\theta = 0°$. This is fully consistent with the experimental observations.

Here the *d* value bears the unit β_{ccc} for the SS mode and β_{aca} for the AS mode. One has $\beta_{ccc}/\beta_{aca} = 2.7$ from the recent empirical treatment and correction of the ratio between the β_{ccc} and β_{aca} values.[46,47] According to the plot in Figure 3, this quantitatively explains the fact that the AS mode cannot be observed in the SFG-VS spectra in both experimental configurations.

The plot also indicates that the pppss mode in configuration II should bear a sign opposite to that of the sspss mode. Because there is no direct interference with other kinds of modes in the ppp spectra, we cannot determine whether the sign is positive or negative from spectral fitting. If any interference effect can be introduced, for example, another molecule is introduced to the interface, then the relative phase between the sspss and pppss modes can be determined. An alternative is to perform the absolute SFG-VS phase measurement as demonstrated by Shen et al.[59] This shall not be a problem for the analysis of the SFG-VS spectra from the vapor/ethanol interface, where interference between different modes exists in the same spectra.

4.2. Orientation of CH_3- Group at Vapor/Ethanol Interface. Here we turn to the experimental configuration dependence of the SFG-VS spectra of the vapor/ethanol interface.

As reported recently,[8,9,62] the vibrational spectral assignment of the ethanol molecule was corrected from the past literature. Now we know that in the SFG-VS spectra from the vapor/ethanol interface the peaks at about 2875, 2930, and 2970 cm^{-1} should be mainly contributed from the CH_3-SS mode, the CH_3-SS-Fermi resonance mode, and the CH_3-AS mode, respectively. From a series of deuterated ethanol SFG-VS studies,[9] it was found that in ssp spectra the symmetric stretching mode of the methylene group also has a small but non-negligible contribution to the 2875 cm^{-1} peak, and the Fermi resonance of the symmetric stretching mode of the methylene group also has a small contribution to the 2970 cm^{-1} peak. A detailed study of the interference effect of these spectral features shall be reported elsewhere.[63] Generally, the apparent features in the SFG-VS spectra of the vapor/ethanol interface discussed below come from the CH_3-SS, CH_3-SS-Fermi, and CH_3-AS modes.

The SFG-VS spectra in two different experimental configurations are shown in Figure 4 (left). Accordingly, the simulation results of the SFG intensity of the CH_3-SS and CH_3-AS modes at the vapor/ethanol interface are also plotted in Figure 4 (right). The simulation of the CH_3-SS-Fermi mode follows the CH_3-SS mode with a slightly larger value for its β_{ccc} value than that of the CH_3-SS mode (because they form a pair of Fermi resonance peaks, and they have the same symmetry and very

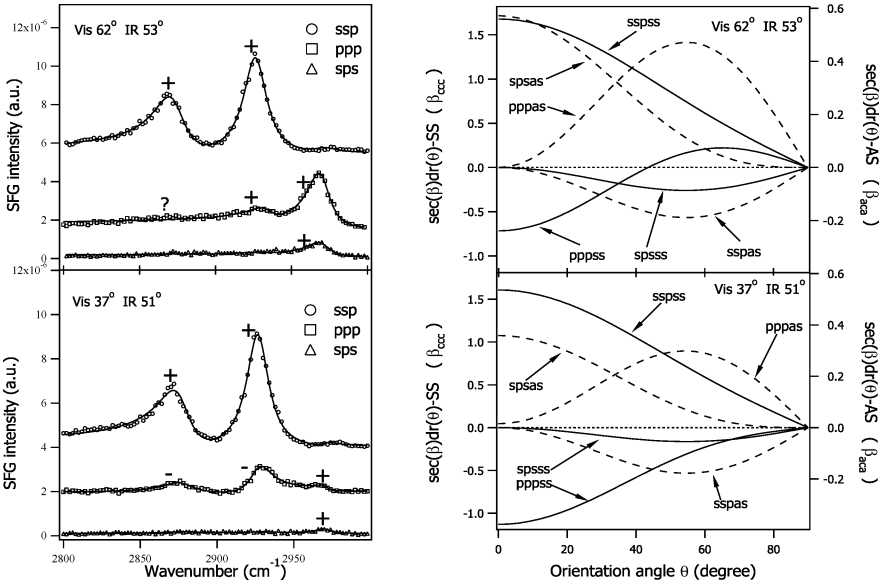

Figure 4. Left: SFG-VS spectra of the vapor/ethanol interface in two experimental configurations. The solid lines are fittings with the Lorentzian line shapes. The phase of each fitted peak is marked near the spectral peak position. Right: simulation of the SFG-VS intensity for the CH_3-SS and the CH_3-AS mode from the vapor/ethanol interface in different orientational angles. The factor sec(β) in eq 1 was included for comparison of the SFG-VS strength and phase in different experimental configurations.

TABLE 2: Parameter *c* and Factor *d* for the Methyl Group at the Vapor/Ethanol Interface in Experimental Configurations I and II

polarization		sspss	pppss	spsss	sspas	pppas	spsas
vis 62, IR 53	*c*	−0.55	1.9	1	1	1.0	∞
	d	0.53	0.39	−0.33	−0.24	0.59	−0.27 (*d*•*c*)
vis 37, IR 51	*c*	−0.55	−3.9	1	1	0.98	∞
	d	0.81	−0.18	−0.33	−0.37	0.60	−0.28 (*d*•*c*)

[a] The notation such as sspss means the ssp polarization combination for the SS mode, and so forth. The *d* value bears the unit β_{ccc} for the SS mode and β_{aca} for the AS mode. The parameters without two effective figures are exact values.

similar parameters). The parameters used in the simulation are the same as those used in the previous work.[8] The refractive index is 1.0 in the air and 1.36 in the bulk ethanol for all of the fundamental laser beams and SFG signal, respectively. The refractive index at the interface is 1.16, calculated according to Zhuang and Shen et al.[10,37] The *c* and *d* values thus calculated are listed in Table 2. The *d* value bears the unit β_{ccc} for the SS mode and β_{aca} for the AS mode. One has $\beta_{ccc}/\beta_{aca} = 0.22$ from the recent empirical treatment and correction of the ratio between the β_{ccc} and the β_{aca} values.[46]

In Figure 4, the relative signs from the spectral fittings are also labeled beside each apparent spectral feature. It is apparent that the sign of the 2930 cm^{-1} peak changed and that for the 2970 cm^{-1} CH_3-AS peak remains unchanged in the ppp polarization combination in the two experimental configurations. The sign of the 2875 cm^{-1} peak cannot be determined explicitly in configuration I, and it is negative relative to the 2970 cm^{-1} peak in configuration II. Because of the existence of the 2970 cm^{-1} peak, the change of the signs of the 2875 and 2930 cm^{-1} peaks can be determined. Such phase change was predicted from the simulation as plotted in Figure 4. It can be seen here that the pppas curve remains positive for all orientational angles (θ) in both experimental configurations, whereas the pppss curve changes sign around $\theta = 42°$ in the first experimental configuration and remains negative in all θ in the second experimental configuration. Therefore, as long as the tilt angle θ of the CH_3- group is larger than 42°, the change of the signs of the CH_3-SS and CH_3-SS-Fermi peaks in the ppp polarization combination can be fully explained. The relative intensities of these peaks in the ppp polarization combination in the two experimental configurations can also be explained from these curves.

Therefore, the phase change of the 2930 cm^{-1} peak in different experimental configurations can be used to determine the orientation of the CH_3- group. In fact, from simulation we learned that there is always an experimental configuration that can make a certain peak in the ppp polarization to change its sign, which is dependent on the molecular orientation. Such information can be used to accurately determine the orientation of the corresponding molecular group at the interface. This is a very important and general conclusion in the SFG-VS experimental configuration analysis.

The orientation of the CH_3- group has been studied in previous SFG-VS studies.[23,25] The conclusions for the tilt angle value were diverse. One gives $\theta \approx 30°$,[25] and another gives $\theta \approx 50°$.[23] Immediately, one can see that the $\theta \approx 30°$ value contradicts with the observed experimental configuration-dependent phase changes of the 2930 cm^{-1} peak discussed above. Therefore, $\theta \approx 50°$ is the one likely to be correct.

Alternatively, both previous reports speculated a relatively broad orientational distribution of the CH_3- group. Because both of these studies were conducted before the correct assignment of the vapor/ethanol interface SFG-VS spectra,[9] a more detailed study on the CH_3- group orientation is warranted. With consideration of the complex interference effects in the SFG-VS spectra, a full study on the SFG-VS intensity analysis and the molecular orientational conformation of the ethanol molecule at the vapor/ethanol interface is going to be reported.[63] In that study, the results were that the tilt angle θ of the CH_3- group is about 45° from the interface normal, and the tilt angle θ of the -CH_2- group is about 80° from the surface normal, with the C−C−O plane perpendicular to the interface plane.

In short conclusion, from the intensity and the phase changes of the SFG-VS spectra in the ppp polarization combination in different experimental configurations, information on the molecular orientation and its distribution can be clearly identified. This is possible because the phase difference between different

vibrational modes can be experimentally obtained and its orientational dependence can be evaluated in different experimental configurations. Such analysis was used successfully in the study of the SFG-VS of the vapor/water interface previously,[13,14] and it worked successfully again for the SFG-VS study of the vapor/ethanol interface here.

4.3. Resolving Spectral Features at Vapor/Ethylene Glycol Interface. The spectral resolving power through the experimental configuration dependence in SFG-VS can be exhibited from the study of the vapor/ethylene glycol interface.

In a previous study, using the SFG-VS polarization selection rules, we concluded that the 2940 cm^{-1} peak in the ssp spectra of the vapor/ethylene glycol interface belongs to the Fermi resonance mode of the CH_2-SS mode, instead of the CH_2-AS mode in other previous studies. We also determined that the CH_2-AS mode is around 2900 cm^{-1}.[7] However, whether the strong 2940 cm^{-1} peak contains some contribution from the CH_2-AS mode or not is still in question[32] because it has been believed that the CH_2-AS mode generally exists at about 2920−2930 cm^{-1} in the vibrational spectroscopy literature.[64−66] Here, the experimental configuration dependence of the SFG-VS spectra of the vapor/ethylene glycol interface in the ppp polarization configuration can help unravel this puzzle.

The SFG-VS spectra of the vapor/ethylene glycol interface were measured in three experimental configurations, that is, configuration I, $\beta_1 = 62°$ and $\beta_2 = 53°$; configuration II, $\beta_1 = 45°$ and $\beta_2 = 55°$; and configuration III, $\beta_1 = 37°$ and $\beta_2 = 51°$.[10] The spectra were shown in Figures 5 and 6. The fitting of the spectra gives a clear phase relationship between the different spectra features, and they are labeled in Figure 5. It is clear that the 2870 and 2940 cm^{-1} peaks in the ppp polarization combination change signs simultaneously when the experimental configuration is changed, whereas the 2900 cm^{-1} peak does not change sign with the experimental configuration. All of these are consistent with the characteristics in our simulations of the CH_2-SS and CH_2-AS mode peaks, respectively. Therefore, one can conclude that the 2940 cm^{-1} peak does not contain contribution from the CH_2-AS mode.

One may notice the asymmetry of the baseline in the SFG-VS spectra in Figure 6, especially for the ppp and sps spectra. This is a common and unique phenomenon due to the spectral interference effect in the coherent spectroscopy. The degree of the baseline asymmetry is determined by many factors, such as the relative phase, the oscillator strength, the peak position, and the peak widths of the interfering spectral features, as well as the sign of the nonresonant contribution.[3,20,43] The significant difference in the baseline between the spectra in different experimental configurations is not surprising for the significant change of the signs and the amplitude of the three contributing spectral features. The reasonably good fittings of those spectra confirmed this fact.

One can expect that the -CH_2- groups cannot rotate freely in each ethylene glycol molecule. A clear indication of this effect is the nonzero intensity of the CH_2-SS mode in the sps polarization combination as shown in Figure 6.[10,32] The full treatment with the nonzero twist angle of the C_{2v} groups was dealt with in the literature, and simulation can be conducted accordingly.[4,10] Simulation of the signs of the CH_2-SS and -CH_2-AS mode peaks in the ppp and sps polarization combination at different -CH_2- orientational angles and twist angles can provide further information about the allowed range of the -CH_2- group twist angle. The same conclusion for a relatively narrow orientation and twist angle distribution can be achieved. According to the simulation, the explicit sign relationship between the spectral features in the ppp and sps polarization combination in different experimental configurations do not allow a broad distribution width for both the orientation and twist angle. It would be too lengthy to present the detail of the simulations here. Instead, here we only describe the major characteristics of the simulation.

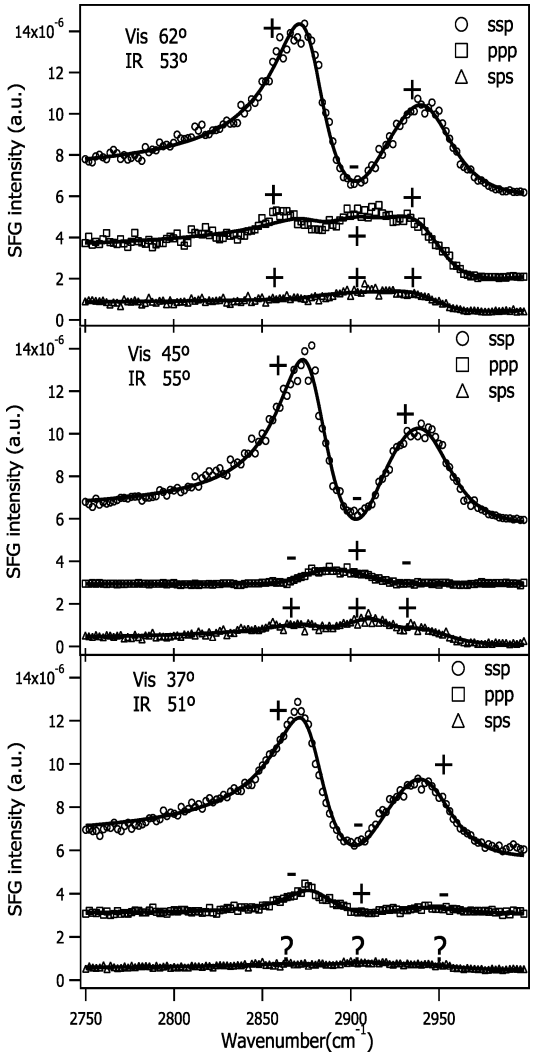

Figure 5. SFG-VS spectra of the vapor/ethylene glycol interface measured in three experimental configurations. The solid curves are fittings with the Lorentzian line shapes. The phase of each fitted peak is marked near the spectral peak position.

One important fact from the simulation is that the CH_2-SS mode has a sign opposite of that of the CH_2-AS mode in the sps polarization combination in all experimental configurations when the twist angle is lager than 50°. In the SFG-VS spectra in the sps polarization combination in all three experimental configurations, the CH_2-SS and CH_2-AS mode peaks bear the same signs. This fact clearly sets the upper limit of the twist angle as 50°. Because the CH_2-SS mode intensities are obviously nonzero in sps, simulation shows that the allowed twist angle should be between 20° and 40°, and the orientational angle is about 35−40°.

These conclusions were also arrived from the fact that the CH_2-SS and CH_2-AS mode peaks in the ppp polarization combination bear the same signs in configuration I and they bear opposite signs in configurations II and III. The simulation showed that the pppss curve changes sign when the tilt angle θ is around 50° when the twist angle is smaller than 50°. When θ is less than 50°, the CH_2-SS and the CH_2-AS mode peaks in

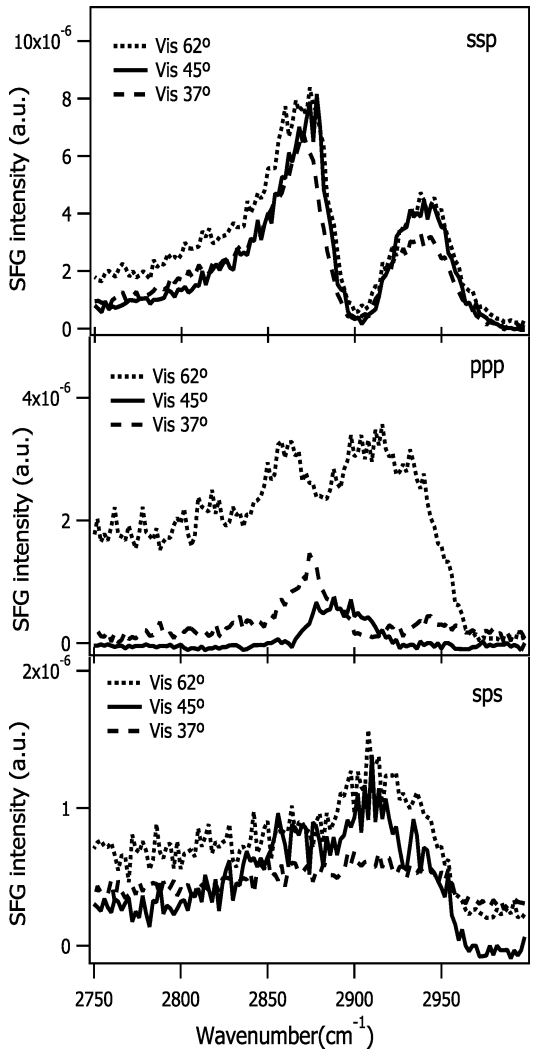

Figure 6. SFG-VS spectra of the vapor/ethylene glycol interface measured in three experimental configurations plotted by the same polarization combination. The different interference effect of the CH_2-SS and CH_2-AS modes in different experimental configurations can be observed clearly.

the ppp polarization combination bear the same signs in configuration I. This clearly sets the upper limit for the tilt angle θ. The details of these comprehensive simulations are to be reported elsewhere.

As one can notice from the details of the SFG-VS spectra in different experimental configurations, the magnitude and phase of the nonresonant contributions to the SFG-VS field is still not very clear. However, this does not change the relative signs and strength of the different spectral features in the same spectrum. Therefore, the above observations are clear demonstrations on how experimental configuration studies can help unravel the contributions from different spectral features in the SFG-VS analysis. Such analysis can be used unambiguously for resolving overlapping spectral features in the SFG-VS spectra.

5. Conclusions

In a recent report on SFG-VS from the vapor/iso-propanol interface by Kataoka et al., two deuterated isopropanol molecules, namely, $(CH_3)_2CDOH$ and $(CD_3)_2CHOH$, along with isopropanol [$(CH_3)_2CHOH$] were used to identify the vibrational peak of the single C−H stretching mode.[67] It was found that in $(CD_3)_2CHOH$ the single C−H stretching mode is at 2895 cm^{-1}, and in $(CH_3)_2CHOH$ the single C−H stretching mode is at 2915 cm^{-1}. The latter value is consistent with our previous report on the SFG-VS polarization spectra of isopropanol with the polarization selection rules.[8] The isotope substitution method in vibrational spectroscopy is undoubtedly very important and useful, but such a big difference in the peak positions of the single C−H stretching mode in $(CD_3)_2CHOH$ and $(CH_3)_2CHOH$ indicates strong coupling between the stretching modes within the isopropanol molecule and thus cast difficulties in using isotope substitution to unravel spectral features in complex molecules, let alone the additional difficulties and expenses to obtain pure isotopic samples. Together with the problems resolved with the recent progresses on using polarization analysis for in situ vibrational spectral assignment,[7−10] we surmise that the experimental configuration analysis in SFG-VS can provide new promises for the application of the polarization analysis method in SFG-VS for vibrational spectral studies.

In this report, we have shown that with the control and simulation of the experimental configuration dependence in SFG-VS, one can obtain unseen spectral features with the optimal experimental configurations, one can use the interference effect in different polarization combinations to obtain information on molecular orientation and orientational distributions, and one can also use the interference effect in different polarization combinations to explicitly resolve spectral features. For each of these capabilities, a clear example with both experimental measurement and theoretical simulation was given in this report. For rotationally isotropic liquid interfaces, control of the experimental configuration can only be through the change of the incident angles of the laser beams. For rotationally anisotropic surfaces, such as the semiconductor or rubbed polymer surfaces, rotation of the sample can also be viewed as a control of the experimental configuration.[50] In any case, more information can be achieved by such control in the SFG-VS experiment.

In a recent report on the SFG-VS study of the air/water interface, four sets of experimental configurations were used to measure the SFG-VS spectra, and the polarization analysis with these spectra helped clarify the fundamental questions on the vibrational spectra assignment, the interface orientational structure, and the orientational motion of the air/water interface.[13,14] There, the most significant feature was that the SFG-VS intensity of the free O−H stretching peak at 3700 cm^{-1} in the ppp polarization combination changed by at least 2 orders of magnitude in different experimental configurations, which helped clear identification of the symmetry category of this spectral feature and also provided a sensitive detection for the molecular orientation of the free O−H orientation at the air/water interface. These studies clearly indicated the usefulness and ability of the experimental configuration analysis in the SFG-VS interface studies.

The effect of the experimental configuration dependence in SFG-VS is particularly significant in the ppp polarization combination because this is the polarization where many different macroscopic susceptibility tensor elements are interfering with each other. Tuning Fresnel factors associated with the different susceptibility tensor elements by changing the experimental configuration can result in rich variations of the SFG-VS spectra in the ppp polarization combination. Thus, novel information on molecular spectroscopy and molecular orientational order can be obtained from synergetic experimental measurement and theoretical simulation. In addition to the polarization selection rules and polarization analysis in the SFG-VS practice, controlling the experimental configuration provides an extra dimension for the SFG-VS technique.

Through detailed molecular symmetry analysis and polarization analysis in different experimental configurations, SFG-VS can certainly become a more powerful tool for both interface studies and vibrational spectroscopy studies. This latter perspective indicates that molecular vibrational spectroscopy can be studied directly with SFG-VS at the molecular interface, which can provide more details on the vibrational spectroscopy than normal Raman and IR spectroscopy. These shall ensure broad applications of the SFG-VS technique. All of these advantages of the SFG-VS over the traditional Raman and IR spectroscopy come from the intrinsic coherent nature of the SFG-VS. These are the same for other intrinsically coherent nonlinear spectroscopic techniques. One may expect more advances in future studies in molecular spectroscopy, structure, and dynamics characterizations through the use of the concepts and methods presented in this work.

Acknowledgment. H.F.W. is thankful for support from the Natural Science Foundation of China (NSFC, No.20373076, No.20425309, No.20533070). Y.G. is also thankful for support from the Natural Science Foundation of China (NSFC, No.20573117, No.20673122).

References and Notes

(1) Shen, Y. R. *Nature* **1989**, *337*, 519−525.
(2) Eisenthal, K. B. *Chem. Rev.* **1996**, *96*, 1343−1360.
(3) Bain, C. D. *J. Chem. Soc. Faraday Trans.* **1995**, *91*, 1281−1296.
(4) Shultz, M. J.; Schnitzer, C.; Baldelli, S. *Int. Rev. Phys. Chem.* **2000**, *19*, 123−153.
(5) Richmond, G. L. *Chem. Rev.* **2002**, *102*, 2693−2724.
(6) Miranda, P. B.; Shen, Y. R. *J. Phys. Chem. B* **1999**, *103*, 3292−3307.
(7) Lu, R.; Gan, W.; Wu, B. H.; Chen, H.; Wang, H. F. *J. Phys. Chem. B* **2004**, *108*, 7297−7306.
(8) Lu, R.; Gan, W.; Wu, B. H.; Zhang, Z.; Guo, Y.; Wang, H. F. *J. Phys. Chem. B* **2005**, *109*, 14118−129.
(9) Gan, W.; Zhang, Z.; Feng, R. R.; Wang, H. F. *Chem. Phys. Lett.* **2006**, *423*, 261−265.
(10) Wang, H. F.; Gan, W.; Lu, R.; Rao, Y.; Wu, B. H. *Int. Rev. Phys. Chem.* **2005**, *24*, 191−256 and references therein.
(11) Rao, Y.; Tao, Y. S.; H. F. Wang, *J. Chem. Phys.* **2003**, *119*, 5226−5236.
(12) Zhang, W. K.; Wang, H. F.; Zheng, D. S. *Phys. Chem. Chem. Phys.* **2006**, *8*, 4041−4052.
(13) Gan, W.; Wu, D.; Zhang, Z.; Feng, R. R.; Wang, H. F. *J. Chem. Phys.* **2006**, *124*, 114705.
(14) Gan, W.; Wu, D.; Zhang, Z.; Feng, R. R.; Wang, H. F. *Chin. J. Chem. Phys.* **2006**, *19*, 20−24.
(15) Chen, H.; Gan, W.; Wu, B. H.; Wu, D.; Zhang, Z.; Wang, H. F. *Chem. Phys. Lett.* **2005**, *408*, 284−289.
(16) Chen, H.; Gan, W.; Wu, B. H.; Wu, D.; Guo, Y.; Wang, H. F. *J. Phys. Chem. B* **2005**, *109*, 8053−8063.
(17) Chen, H.; Gan, W.; Lu, R.; Guo, Y.; Wang, H. F. *J. Phys. Chem. B* **2005**, *109*, 8064−8075.
(18) (a) Johnson, C. M.; Tyrode, E.; Baldelli, S.; Rutland, M. W.; Leygraf, C. *J. Phys. Chem. B* **2005**, *109*, 321−328. (b) Tyrode, E.; Johnson, C. M.; Baldelli, S.; Leygraf, C.; Rutland, M. W. *J. Phys. Chem. B* **2005**, *109*, 329−341.
(19) Du, Q.; Superfine, R.; Freysz, E.; Shen, Y. R. *Phys. Rev. Lett.* **1993**, *70*, 2313−2316.
(20) Brown, MacG.; Raymond, E. A.; Allen, H. C.; Scatena, L. F.; Richmond, G. L. *J. Phys. Chem. A* **2000**, *104*, 10220−10226.
(21) Liu, Y.; Messmer, M. C. *J. Phys. Chem. B* **2003**, *107*, 9774−9779.
(22) Wang, J.; Chen, C. Y.; Buck, S. M.; Chen, Z. *J. Phys. Chem. B* **2001**, *105*, 12118−12125.
(23) Sung, J.; Park, K.; Kim, D. *J. Korean Phys. Soc.* **2004**, *44*, 1394−1398.
(24) Superfine, R.; Huang, J. Y.; Shen, Y. R. *Phys. Rev. Lett.* **1991**, *66*, 1066−1069.
(25) Stanners, C. D.; Du, Q.; Chin, R. P.; Cremer, P.; Somorjai, G. A.; Shen, Y. R. *Chem. Phys. Lett.* **1995**, *232*, 407−413.
(26) Wolfrum, K.; Graener, H.; Laubereau, A. *Chem. Phys. Lett.* **1993**, *213*, 41−46.
(27) Wang, C. Y.; Groenzin, H.; Shultz, M. J. *J. Phys. Chem. B* **2004**, *108*, 265−272.
(28) Wang, C. Y.; Groenzin, H.; Shultz, M. J. *J. Am. Chem. Soc.* **2004**, *126*, 8094−8095.
(29) Ma, G.; Allen, H. C. *J. Phys. Chem. B* **2003**, *107*, 6343−6349.
(30) Huang, J. Y.; Wu, M. H. *Phys. Rev. E* **1994**, *50*, 3737−3746.
(31) Sung, J.; Kim, D. *J. Phys. Chem. C* **2007**, *111*, 1783−1787.
(32) Hommel, E. L.; Merle, J. K.; Ma, G.; Hadad, C. M.; Allen, H. C. *J. Phys. Chem. B* **2005**, *109*, 811−818.
(33) Dick, B.; Gierulski, A.; Marowsky, G.; Reider, G. A. *Appl. Phys. B* **1985**, *38*, 107−116.
(34) Hollering, R. W. J. *J. Opt. Soc. Am. B* **1991**, *8*, 374−377.
(35) Tanaka, Y.; Lin, S.; Aono, M.; Suzuki, T. *Appl. Phys. B* **1999**, *68*, 713−718.
(36) Gan, W.; Wu, B. H.; Chen, H.; Guo, Y.; Wang, H. F. *Chem. Phys. Lett.* **2005**, *406*, 467−473.
(37) Zhuang, X.; Miranda, P. B.; Kim, D.; Shen, Y. R. *Phys. Rev. B* **1999**, *59*, 12632−12640.
(38) Hermann, H.; Lvovsky, A. I.; Wei, X.; Shen, Y. R. *Phys. Rev. B* **2002**, *66*, 205110.
(39) Hatch, S. R.; Polizzotti, R. S.; Dougal, S.; Rabinowitz, P. *J. Vac. Sci. Technol.* **1993**, *11*, 2232−2238.
(40) Messmer, M. C.; Conboy, J. C.; Richmond, G. L. *J. Am. Chem. Soc.* **1995**, *117*, 8039−8040.
(41) Conboy, J. C.; Messmer, M. C.; Richmond, G. L. *J. Phys. Chem.* **1996**, *100*, 7617−7622.
(42) Felderholf, B. U.; Bratz, A.; Marowsky, G.; Roders, O.; Sieverdes, F. *J. Opt. Soc. Am. B* **1993**, *10*, 1824−1833.
(43) Löbau, J.; Wolfrum, K. *J. Opt. Soc. Am. B* **1997**, *14*, 2505−2512.
(44) Bloembergen, N.; Pershan, P. S. *Phys. Rev.* **1962**, *128*, 606−622.
(45) Yang, Y. J.; Pizzolatto, R. L.; Messmer, M. G. *J. Opt. Soc. Am. B* **2000**, *17*, 638−645.
(46) Wu, H.; Zhang, W. K.; Gan, W.; Cui, Z. F.; Wang, H. F. *J. Chem. Phys.* **2006**, *125*, 133203.
(47) Wu, H.; Zhang, W. K.; Gan, W.; Cui, Z. F.; Wang, H. F. *Chin. J. Chem. Phys.* **2006**, *19*, 187−189.
(48) Wang, H. F. *Chin. J. Chem. Phys.* **2004**, *17*, 362−368.
(49) Michl, J.; Thulstrup, E. W. *Spectroscopy with Polarized Light*; VCH Publishers Inc: New York, 1995.
(50) Wei, X.; Hong, S. C.; Zhuang, X. W.; Goto, T.; Shen, Y. R. *Phys. Rev. E* **2000**, *62*, 5160−5172.
(51) Goldstein, H. *Classic Mechanics*; Addison-Wesley Publisishing Company, Inc.: Boston, MA, 1980; p 147.
(52) Wang, H. F. *Chin. J. Chem. Phys.* **2004**, *17*, 362−368.
(53) Watanabe, N.; Yamamoto, H.; Wada, A.; Domen, K.; Hirose, C. *Spectrochim. Acta, Part A* **1994**, *50*, 1529−1537.
(54) Du, Q.; Freysz, E.; Shen, Y. R. *Phys. Rev. Lett.* **1994**, *72*, 238−241.
(55) (a) Lu, R.; Gan, W.; Wang, H. F. *Chin. Sci. Bull.* **2003**, *48*, 2183−2187. (b) Lu, R.; Gan, W.; Wang, H. F. *Chin. Sci. Bull.* **2004**, *49*, 899.
(56) Wang, J.; Clarke, M. L.; Chen, Z. *Anal. Chem.* **2004**, *76*, 2159−2167.
(57) Shen, Y. R.; Ostroverkhov, V. *Chem. Rev.* **2006**, *106*, 1140−1154.
(58) Ji, N.; Ostroverkhov, V.; Belkin, M.; Shiu, Y. J.; Shen, Y. R. *J. Am. Chem. Soc.* **2006**, *128*, 8845−8848.
(59) Superfine, R.; Huang, J. Y.; Shen, Y. R. *Opt. Lett.* **1990**, *15*, 1276−1278.
(60) Chen, W. G.; Braiman, M. S. *Photochem. Photobiol.* **1991**, *54*, 905−910.
(61) Zhang, J. P.; Inaba, T.; Watanabe, Y.; Koyama, Y. *Chem. Phys. Lett.* **2000**, *331*, 154−162.
(62) Yu, Y. Q.; Lin, k.; Zhou, X. G.; Wang, H.; Liu, S. L.; Ma, X. X. *J. Phys. Chem. C* **2007**, *111*, 8971−8978.
(63) Gan, W.; Zhang, Z.; Feng, R.-r.; Wang, H.-f. *J. Phys. Chem. C* **2007**, *111*, 8726−8738.
(64) Colthup, N. B.; Daly, L. H.; Wiberley S. E. *Introduction to Infrared and Raman Spectroscopy*; Academic Press Inc.: San Diego, CA, 1990.
(65) Bellamy, L. J. *The Infrared Spectra of Complex Molecules*; Chapman and Hall: London, 1975.
(66) Herzberg, G. *Molecular Spectra and Molecular Structure II: Infrared and Raman Spectra of Polyatomic Molecules*; D. Van Nostrand Co., Inc.: Princeton, NJ, 1945; Chapter V.
(67) Kataoka, S.; Cremer, P. S. *J. Am. Chem. Soc.* **2006**, *128*, 5516−5522.